Reaction Dynamics and Vibrational Spectroscopy of CH_3D Molecules with Both C−H and C−D Stretches Excited†

Christopher J. Annesley, Andrew E. Berke, and F. Fleming Crim*

Department of Chemistry, University of Wisconsin—Madison, Madison, Wisconsin 53706

Received: May 2, 2008; Revised Manuscript Received: June 9, 2008

State-resolved reactions of CH_3D molecules containing both C−H and C−D stretching excitation with Cl atoms provide new vibrational spectroscopy and probe the consumption and disposal of vibrational energy in the reactions. The vibrational action spectra have three different components, the combination of the C−H symmetric stretch and the C−D stretch ($\nu_1 + \nu_2$), the combination of the C−D stretch and the C−H antisymmetric stretch ($\nu_2 + \nu_4$), and the combination of the C−D stretch and the first overtone of the CH_3 bend ($\nu_2 + 2\nu_5$). The simulation for the previously unanalyzed ($\nu_2 + \nu_4$) state yields a band center of $\nu_0 = 5215.3$ cm^{-1}, rotational constants of $A = 5.223$ cm^{-1} and $B = 3.803$ cm^{-1}, and a Coriolis coupling constant of $\zeta = 0.084$. The reaction dynamics largely follow a spectator picture in which the surviving bond retains its initial vibrational excitation. In at least 80% of the reactive encounters of vibrationally excited CH_3D with Cl, cleavage of the C−H bond produces CH_2D radicals with an excited C−D stretch, and cleavage of the C−D bond produces CH_3 radicals with an excited C−H stretch. Deviations from the spectator picture seem to reflect mixing in the initially prepared eigenstates and, possibly, collisional coupling during the reaction.

I. Introduction

The reaction of methane with chlorine is a model system for studying the ability of vibrational excitation to control chemical pathways.[1–16] Studies of the reaction yield, product identities, and product excitations for reaction of the partially deuterated isotopologues, CH_3D,[2–5] CH_2D_2,[8,9] and CHD_3,[8] with Cl have demonstrated that vibrational excitation of a C−H or C−D bond leads to preferential cleavage of that bond and that vibrational energy initially in a bond that does not break largely survives as excitation of the products. These studies have also shown that vibrational states having similar energies but corresponding to different nuclear motions can have quite different reactivities, an example of mode-selective chemistry.[17] One comparison between CH_3D molecules with either the symmetric or antisymmetric C−H stretch excited shows about a 7-fold greater reactivity for molecules with energy in the symmetric C−H stretching state.[3] Reactions of either CH_3D[5] or CH_2D_2[8] prepared in molecular eigenstates that contain excitation in two of the C−H oscillators clearly demonstrate the survival of excitation in the unbroken bond by producing radicals with a quantum of C−H stretching excitation intact. In contrast, preparation of states with all of the excitation in one bond leads to a radical product with no C−H stretching vibration.

All of these measurements support a simple spectator picture in which the surviving bond is largely unchanged in the reaction. Thus, in reactions involving either C−H or C−D stretching excitation, the hydrogen isotope in the unexcited bond appears in the radical product, and in reactions with vibrational excitation in two identical bonds, the bond that survives retains its vibrational energy. Here we study these two aspects of the simple spectator picture together by preparing a combination state of CH_3D that has a quantum of excitation in both a C−H bond and the C−D bond and observing the products from reaction with Cl atoms,

$$Cl + CH_3D(v_{CH}, v_{CD}) \rightarrow \begin{cases} CH_3(v'_{CH}) + DCl \\ CH_2D(v'_{CD}) + HCl \end{cases}$$

There is only a single C−D stretching vibration in CH_3D, denoted as the normal mode ν_2, but the three equivalent C−H bonds result in three vibrational states, the nondegenerate symmetric C−H stretching vibration, ν_1, and the degenerate antisymmetric C−H stretching vibration, ν_4. Thus, the combination states we excite are nominally $\nu_1 + \nu_2$, which has A_1 vibrational symmetry in the C_{3v} point group of CH_3D, and $\nu_2 + \nu_4$, which has E vibrational symmetry. There is also a Fermi resonance between the symmetric C−H stretch, ν_1, and the first overtone of the degenerate CH_3 bend, $2\nu_5$, that gives the transition to the $\nu_2 + 2\nu_5$ state transition strength by mixing it with the $\nu_1 + \nu_2$ state.

Figure 1 shows a sketch along the reaction coordinate for breaking either the C−H or C−D bonds along with some of the vibrational states of CH_3D and of the radical products for the two channels. We excite different combination bands using infrared laser light and detect the radical reaction products in various quantum states using resonant enhanced multiphoton ionization (REMPI) to study the bond selectivity, relative reactivity, and product energy partitioning. Because we have previously studied CH_3D molecules with two stretching quanta in the same C−H bond and in two different C−H bonds,[5] we can now compare their behavior with that of molecules having one quantum in a C−H stretch and one quantum in a C−D stretch.

II. Experimental Approach

The experimental approach is very similar to the one we have used previously,[1,2,5] and although the apparatus is largely rebuilt, many of the details are the same. We expand a 600 Torr, 1:1:5 mixture of Cl_2, CH_3D, and He through a 0.4 mm pulsed valve along the axis of a differentially pumped Wiley-McClaren[18]

† Part of the "Stephen R. Leone Festschrift".

* Corresponding author. E-mail: fcrim@chem.wisc.edu.

10.1021/jp803901p CCC: $40.75
Published on Web 08/05/2008

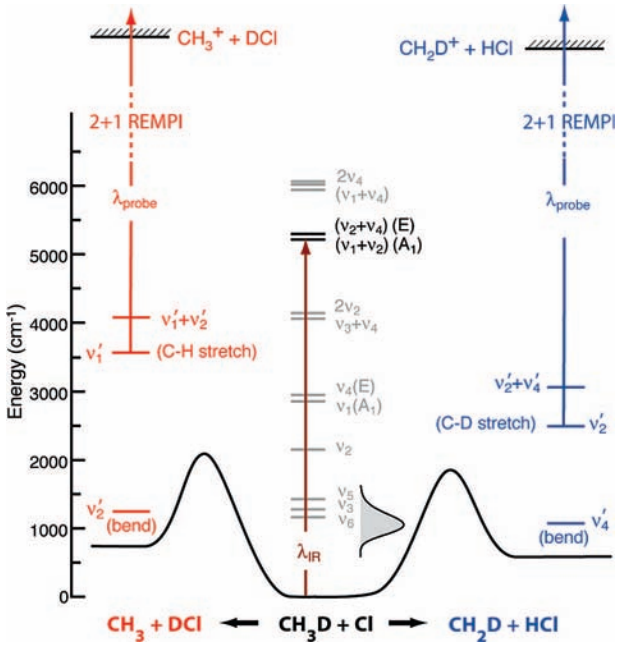

Figure 1. Sketch of the energy profiles along the reaction coordinate for producing CH_3 + DCl and CH_2D + HCl in the reaction of CH_3D with Cl. The energy levels in the center of the figure are those for CH_3D with a vertical arrow indicating the infrared excitation used in these experiments. The energy levels on the left mark the C−H stretch (ν_1'), the bend (ν_2') state and the combination of the two ($\nu_1' + \nu_2'$) in CH_3. The energy levels on the right mark the C−D stretch (ν_2'), the bend (ν_4') state and the combination of the two ($\nu_2' + \nu_4'$) in CH_2D. The shaded curve shows the nominal distribution of center-of-mass collision energies in the experiment.

time-of-flight mass spectrometer. These conditions produce a rotational temperature of about 120 K for CH_3D molecules in the expansion. In the ionization region, a 10 mJ, 0.06 cm^{-1} pulse of infrared light vibrationally excites some of the CH_3D molecules, and 20 ns later a 6 mJ pulse of 355 nm photolysis light dissociates Cl_2 to form Cl atoms. After 200 ns, during which some of the vibrationally excited molecules react, a 2−4 mJ pulse of 333 nm light ionizes the product radicals by (2 + 1) REMPI through either the $3p^2B_1$ Rydberg state for CH_2D[19] or the $3p^2$ A_1'' Rydberg state for CH_3,[20] and a multichannel plate detects the ions as they arrive at the end of the flight tube. We have reduced the probe power density from that of earlier experiments by using a 75 cm focal length lens to avoid background from nonresonant multiphoton processes. Because there is a significant thermal reaction of molecules without added vibrational excitation, we use a shutter in the infrared beam and detect the signal with and without the infrared light present for intervals of 1 or 2 s to subtract the thermal background from the vibrationally enhanced reaction. A small amount of light from the infrared beam excites CH_3D molecules in a photoacoustic cell to provide a simultaneous room temperature absorption spectrum.

III. Results and Discussion

A. Vibrational Spectroscopy. The vibrational action spectra we obtain by monitoring a reaction product as a function of the infrared excitation wavelength provide two types of information. The first is spectroscopic, allowing us to obtain constants for the vibrational transitions in the combination region, and the second is dynamic, allowing us to determine the relative reactivity of molecules with different vibrations excited. There are relatively few studies of the combination states involving the C−H and C−D stretch,[21−24] but they are interesting for examining the spectator picture of the reaction dynamics. Table 1 gives the band centers and other spectroscopic constants for the combination of the C−H symmetric stretch and the C−D stretch ($\nu_1 + \nu_2$), the combination of the C−D stretch and the C−H antisymmetric stretch ($\nu_2 + \nu_4$), and the combination of the C−D stretch and the bend overtone ($\nu_2 + 2\nu_5$) that we consider. Previous high resolution studies provide rotational constants for the first and third combinations,[24] which have A_1 symmetry, but not for the second, E symmetry state.

TABLE 1: Spectroscopic Constants for Simulation of the Action Spectrum[a]

	ν_0 (cm^{-1})	A (cm^{-1})	B (cm^{-1})	ζ
ground state[b]		5.250821	3.880195	
$\nu_2 + \nu_4$ (E)[c]	5215.3(9)	5.223(50)	3.803(50)	0.084(2)
$\nu_1 + \nu_2$ (A_1)[d]	5165.04(3)	5.174(50)[e]	3.8602(32)	
$\nu_2 + 2\nu_5$ (A_1)[d]	5103.63(12)	5.251[f]	3.9905(18)	

[a] The numbers in parentheses are the uncertainties in the last digits of the reported value. [b] Reference 25. [c] This work. [d] Reference 24. [e] This value corrects an apparent misprint in ref 24. The difference in the excited state and ground state A rotational constants is $A' - A'' = -0.077$ although ref 24 gives the opposite sign. [f] Reference 24 reports the A rotational constants to be the same in the ground and excited state.

Figure 2a shows the room temperature photoacoustic spectrum along with a simulation using the known constants for the ground state[25] and the two A_1-symmetry states[24] and our best-fit values for the E state. These values are not from a fit to the congested photoacoustic spectrum but from a fit to the simpler, low temperature action spectra shown in Figure 2b,c. The action spectrum in Figure 2b comes from monitoring CH_2D with a quantum of C−D stretching excitation (ν_2'), and the action spectrum in Figure 2c comes from monitoring CH_3 with a quantum of C−H stretching excitation (ν_1'). In both cases, the simulation is the sum of the three components shown in the lower portion of Figure 2b although the weighting of the components is different for the two products, as described below.

Table 1 gives the parameters used in the simulation of the three components. Because the Coriolis coupling is important in the degenerate E state, we also adjust its value to best reproduce the positions of the E-symmetry transitions.[26,27] Estimates of the rotational and Coriolis coupling constants for the combination states obtained by scaling the values for the fundamentals[23,26] do not agree well with the observations for either the A_1 or the E states, likely reflecting interactions with still other states.[24] There are a few transitions that the simulation does not recover along with some anomalous intensities, which come from isolated perturbations and a few transitions that belong to other nearby states. We have adjusted the relative intensities of each of the three components to obtain the best simulation, as described below, and have used a rotational temperature of $T_{rot} = 120$ K for all of the states. The assumptions that a temperature characterizes the populations of different symmetric-top states in the expansion and that it is the same for all three vibrational components are only rough approximations to the actual situation. Despite all of these approximations, the relatively simple simulation reproduces the observed low temperature action spectra (Figure 2b,c) satisfactorily. These simulations allow us to identify the features we excite in measurements of the relative product state populations and to extract relative reactivities for the different vibrational states.

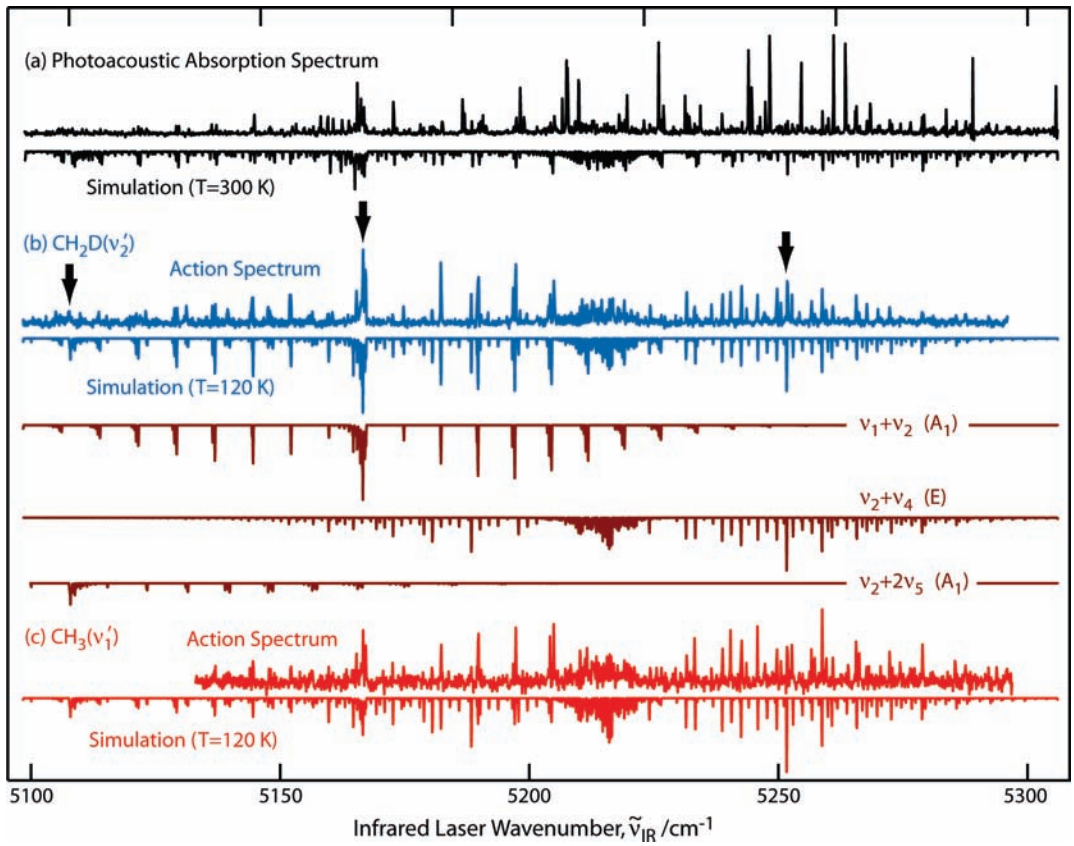

Figure 2. Spectra of CH_3D in the region of combination states containing a quantum of C−H and a quantum of C−D stretch. (a) Photoacoustic absorption spectrum and a simulation of the spectrum at $T = 300$ K. (b) Action spectrum obtained monitoring the $CH_2D(\nu_2')$ product of the reaction of CH_3D with Cl and a simulation of the spectrum at $T = 120$ K. The traces below the simulation show the three components of the spectrum, $\nu_1 + \nu_2$, $\nu_2 + \nu_4$, and $\nu_2 + 2\nu_5$, with amplitudes adjusted to reproduce best the action spectrum. The vertical arrows show the excitation wavelengths used to obtain the product REMPI spectra shown in Figure 3. (c) Action spectrum obtained monitoring the $CH_3(\nu_1')$ product of the reaction of CH_3D with Cl and a simulation of the spectrum at $T = 120$ K. The same components as shown in (b) but with different amplitudes go into the simulation.

B. Product States. Fixing the vibrational excitation laser on a feature in the vibrational spectrum and detecting the relative populations of different vibrational states of the radical products, CH_2D or CH_3, allows us to probe the extent to which simple ideas about preserving excitation in nonreacting bonds describe the reaction. Figure 3 shows the primary data from which we obtain relative populations of different product states. The points are the (2 + 1) REMPI signal for either CH_2D (Figure 3a) or CH_3 (Figure 3b) as a function of the two-photon energy in the ionization. The mass sensitive detection distinguishes the two products, and transitions for each different product vibrational state occur at slightly different wavelengths, as indicated by the labels in the figure. The data in the figure are for two different initial vibrations of CH_3D: the A_1-symmetry combination of the symmetric C−H stretch and the C−D stretch ($\nu_1 + \nu_2$) or the E-symmetry combination of the C−D stretch and antisymmetric C−H stretch ($\nu_2 + \nu_4$). We obtain similar, but lower quality, data following excitation of the A_1-symmetry combination of the C−D stretch and the C−H bend overtone $\nu_2 + 2\nu_5$, which apparently has a Fermi resonance with the $\nu_1 + \nu_2$ combination.

The data for the CH_2D product show that the three most populated states are the C−D stretch (ν_2'), its combination with a bending vibration ($\nu_2' + \nu_4'$), and the bending vibration alone (ν_4'). (This bending vibration is a large amplitude, out-of-plane motion that is analogous to the umbrella bend in CH_3.[19]) Although there is not a previous observation of the C−D stretching vibration (ν_2') in CH_2D, we are able to identify it as the transition lying (51 ± 2) cm^{-1} below the transition to the origin by comparing the calculated frequencies of the radical and the cation, as we did previously in assigning the C−H stretch.[5] There is some indication of a depletion of the ground state product for excitation of the A_1-symmetry vibration, but the large fluctuations we observe on that transition, primarily because of subtracting the background from the thermal reaction, add a great deal of uncertainty. The smooth curves in the figure are Lorentzian fits through the features that we integrate to obtain the areas of the transitions. The size of the ion signal suggests that the yield of the CH_3 fragment is a few times smaller than that of CH_2D, in keeping with the greater number of C−H bonds to break and the kinetic isotope effect, but we cannot make a definitive comparison without knowing the ionization cross section and detection efficiency for the different products. The lower portion of the figure shows that most of the CH_3 fragments have a quantum of symmetric C−H stretching (ν_1') excitation along with a small population of the combination with the bend ($\nu_1' + \nu_2'$). The data shown in Figure 3 and discussed below are taken with the vibrational excitation laser fixed at the points marked with vertical arrows on the action spectrum of Figure 2, but excitation on other transitions produces similar results.

Figure 4 summarizes the relative yields of each of the CH_2D and CH_3 radical states from the reaction of $CH_3D(\nu_1+\nu_2)$ and of $CH_3D(\nu_2+\nu_4)$. The bars give the fractional areas under each transition in the REMPI excitation spectra, and the uncertainties shown in the figure reflect the variations we observe in our data.

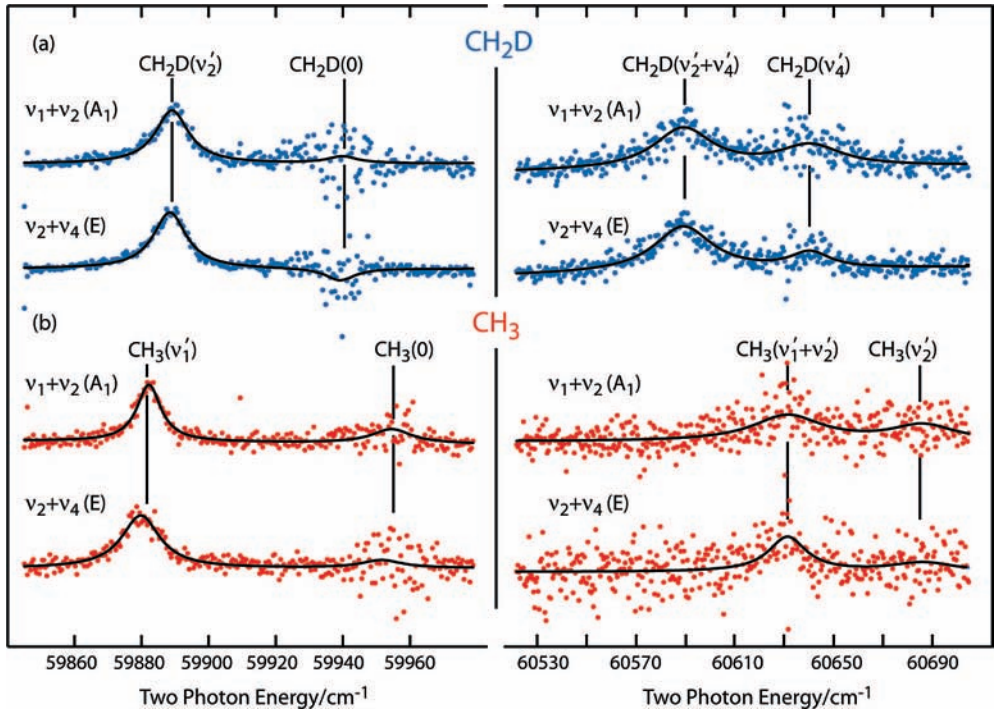

Figure 3. (2 + 1) REMPI excitation spectra of the products of the reaction of Cl with CH_3D containing a quantum of C−H and a quantum of C−D stretching excitation. (a) Spectra of CH_2D obtained for reaction of $CH_3D(\nu_1+\nu_2)$ (upper trace) and $CH_3D(\nu_2+\nu_4)$ (lower trace). The vertical lines mark transitions from different vibrational states of the CH_2D product. The smooth black lines are Lorentzian curves fit to the data. (b) Spectra of CH_3 obtained for reaction of $CH_3D(\nu_1+\nu_2)$ (upper trace) and $CH_3D(\nu_2+\nu_4)$ (lower trace). The vertical lines mark transitions from different vibrational states of the CH_3 product. The smooth black lines are Lorentzian curves fit to the data.

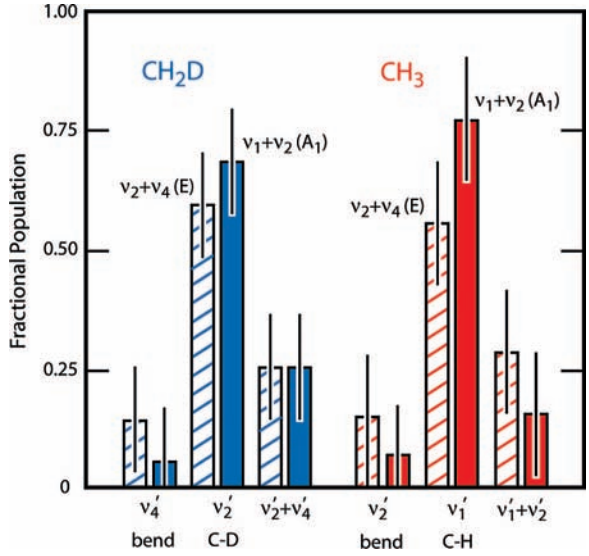

Figure 4. Relative populations of the vibrational states of the radical product of the reaction of Cl with CH_3D containing a quantum of C−H and a quantum of C−D stretch. The bars show the relative populations for reaction of $CH_3D(\nu_1+\nu_2)$ (solid bar) and $CH_3D(\nu_2+\nu_4)$ (hatched bar). The CH_2D products (shown on the left) are formed with a quantum of C−D stretch (ν_2'), a quantum of bend (ν_4'), or a combination of the two ($\nu_2' + \nu_4'$). The CH_3 products (shown on the right) are formed with a quantum of C−H stretch (ν_1'), a quantum of bend (ν_2'), or a combination of the two ($\nu_1' + \nu_2'$).

Our analysis uses diagonal probe transitions, which have the same number of vibrational quanta in the upper and lower states. Thus, although we do not know the Franck−Condon factors for all of the transitions, it is reasonable to assume that they are similar enough that we can use the integrated areas of the transitions as a measure of the relative populations of the different states within one of the isotopically distinct products. However, we cannot make quantitative comparisons between the populations for the two different channels.

The left-hand side of Figure 4 shows the results for the CH_2D products from cleavage of the C−H bond. One useful comparison is between the product state populations shown here for the reaction of CH_3D molecules having excitation in *both* the C−H and the C−D stretches and those for the reaction of CH_3D having *only* the C−H stretch excited. Reactions of CH_3D with either one or two quanta of C−H stretch excited largely follow a spectator picture.[4,5] In the case of CH_3D states that initially have vibrational energy in two different C−H bonds, a quantum of C−H stretching excitation survives in the CH_2D product, but in the case of initial excitation in only one bond, there is no C−H stretching excitation in the product. In all of the cases, however, some of the CH_2D radicals are born with a quantum of bending excitation (ν_4'),[5] which likely arises from the geometry change in going from the tetrahedral reactant to the planar methyl radical product. Thus, for example, the products of the reaction of $CH_3D(\nu_4)$, which has the antisymmetric C−H stretch excited, are primarily $CH_2D(0)$ and $CH_2D(\nu_4')$.[5] By analogy, a spectator picture suggests that reaction of $CH_3D(\nu_2+\nu_4)$, which has the antisymmetric C−H stretch *and* the C−D stretch excited, should populate the same states in the product *along with* a quantum of C−D stretch excitation. Indeed, $CH_2D(\nu_2')$, which has a quantum of C−D stretch excitation, and $CH_2D(\nu_2'+\nu_4')$, which has a quantum of C−D stretch excitation combined with the bend, account for at least 80% of the products of the reaction of the combination states.

The remaining CH_2D products are born with a single quantum of bending excitation (ν_4'), which does not fit with a strict spectator picture. The likely origin of the bending excitation is mixing in the initially prepared eigenstate or during the reactive collision. Although we name these vibrational eigenstates by

their dominant zero-order state character such as C−H or C−D stretching, they contain some admixture of other zero-order states that influence the populations of the products states. In particular, complete analysis of the fundamental transitions in CH_3D requires inclusion of several bending modes in high order polyads.[28] The same behavior is likely for the states we excite, and those couplings populate product states that have bending modes rather than the nominal spectator modes excited. It is also possible that the interaction with the incoming Cl collisionally mixes these same states although we have not found that effect to be large in other cases.

Our observing a small amount of reaction of $CH_3D(\nu_2+2\nu_5)$ illustrates the consequence of strong mixing of states most clearly. Although the designation corresponds to a quantum of C−D stretch and two quanta of a bending vibration, the state actually contains significant C−H stretch character because of the Fermi resonant interaction that couples the C−H symmetric stretch (ν_1) and the bending overtone ($2\nu_5$). The mixing is obvious in the spectra in Figure 2, where the $\nu_2+2\nu_5$ combination band appears as a weak set of transitions with the characteristic rotational structure for an A_1 vibrational state. There are dynamical consequence of this mixing in both reaction channels. The reaction to cleave the C−H bond is possible because of the C−H stretching character of the $\nu_2+2\nu_5$ state, and breaking the C−H bond forms $CH_2D(\nu_2')$ in which a quantum of C−D stretching excitation survives as a spectator, following the same pattern as the other C−H stretch excited states illustrated in Figure 4. The reaction to cleave the C−D bond is perhaps even more interesting. It forms methyl radicals with a quantum of C−H stretching excitation, $CH_3(\nu_1')$, as shown by the small transitions in the action spectrum in Figure 2c. Thus, despite nominally having CH_3 bend character, $CH_3D(\nu_2+2\nu_5)$ reacts to form the C−H stretch excited product, in keeping with the mixing of C−H stretch and CH_3 bending vibrations.

The small signals for the reactions producing CH_3 make the uncertainties in the relative product state populations large. The formation of any CH_3 is significant because its presence shows that either the C−H or the C−D bond can react when both are excited in CH_3D. Both the larger barrier arising from the difference in zero-point energies and the lower energy in one quantum of C−D stretch seem to make cleavage of that bond less efficient. The results on the right of Figure 4 show that the spectator picture describes the CH_3 channel fairly well. The reaction primarily produces $CH_3(\nu_1')$, which has the symmetric C−H stretch excited, along with some CH_3 having a combination of C−H stretch and bending excitation ($\nu_1'+\nu_2'$).

IV. Relative Reaction Probabilities

Knowing the identities of the most important product states allows us to make a rough estimate of the *relative* state-to-state reaction probabilities for the different initial vibrational states using the absorption spectrum of Figure 2a and the action spectra of Figure 2b,c. The intensity of a feature in the photoacoustic absorption spectrum reflects the probability of making a transition to one of the three CH_3D vibrational states, $\nu_1+\nu_2$, $\nu_2+\nu_4$, and $\nu_2+2\nu_5$, but the intensities in the action spectrum reflect both the probability of that excitation *and* the probability that the prepared state reacts to form products in the observed state. Thus, the ratio of the scaling factor for each component in the simulation of the action spectrum to the scaling factor for that same component in the absorption spectrum is an estimate of the relative reaction probability. Table 2 collects those ratios determined from action spectra monitoring the two most populated states of the CH_2D product, ν_2' and $\nu_2'+\nu_4'$, and the most populated state of the CH_3 product, ν_1'. Because this analysis does not permit comparison of different product states, we arbitrarily set the ratio to unity for $CH_3D(\nu_1+\nu_2)$ in each case. The small differences in the relative reactivities of the states lie within the uncertainties in most cases. The one possible exception is production of CH_3, in which $CH_3D(\nu_2+\nu_4)$ seems more reactive than the other two states.

TABLE 2: Relative State-to-State Reaction Probabilities for Different CH_3D Vibrations[a]

	CH_3D reactant		
product	$\nu_1+\nu_2$ (A_1)	$\nu_2+\nu_4$ (E)	$\nu_2+2\nu_5$ (A_1)
$CH_2D(\nu_2')$	1	0.7 ± 0.3	0.6 ± 0.4
$CH_2D(\nu_2'+\nu_4')$	1	0.7 ± 0.6	
CH_3 (ν_1')	1	2.1 ± 0.3	1.0 ± 0.4

[a] The relative reactivities are the ratio of the scaling factor between the components in the simulation of the action spectrum and those for the simulation of the photoacoustic absorption spectrum. The ratio for each product state is normalized to unity for $CH_3D(\nu_1+\nu_2)$.

A perplexing aspect of these results is the similarity in the relative reactivity of the A_1 and the E vibrational states, which stands in sharp contrast to the situation for excitation of single C−H stretching vibrations.[3] In that case, the excitation of the symmetric C−H stretching state (ν_1) accelerates the reaction about seven times more effectively than excitation of the antisymmetric C−H stretching state (ν_4). The critical effect seems to be the perturbation of the initially excited vibration during the collision. For the unfavorable case of molecules with the antisymmetric stretch excited, the perturbation sequesters the excitation in C−H stretches that are distant from the incoming atom and, thus, reduces the reactivity. That behavior does not occur in the case of two excited C−H bonds, apparently because the perturbation does not isolate both of them.[5,29] There are indeed two potentially reactive bonds in the combination states we excite, but there are no strong correlations between the symmetry of the initially excited C−H stretching component and the reactivity of the state. This insensitivity may be another consequence of mixing bending vibrations into the initially prepared eigenstates.

V. Conclusions

Preparing CH_3D molecules in eigenstates that contain both a quantum of C−H stretching excitation and a quantum of C−D stretching excitation and then reacting them with Cl atoms shows that a simple spectator model describes most aspects of the energy consumption and disposal in H- and D-atom abstraction reactions. In agreement with the spectator picture, at least 80% of the vibrationally excited molecules react to form a radical in which a surviving bond, be it a C−H bond or a C−D bond, retains its initial vibrational excitation. One deviation from a strict spectator picture is the production of about 20% of the CH_2D radicals with only bending excitation and, thus, no vibrational excitation carried through in the C−D bond. Coupling in the initially prepared eigenstate, which mixes in states that can have the initial C−D excitation replaced with bending excitation, and collisional mixing of the states are possible origins of this behavior. Another example of intramolecular coupling influencing the reactivity is the behavior of the combination state, $\nu_2+2\nu_5$, which is nominally a mixture of the C−D stretch and the first overtone of the C−H bend. This state reacts to cleave the C−H bond even though bending

vibration should not promote that reaction. However, a Fermi resonance interaction between $2\nu_5$ and the symmetric C−H stretch, ν_1, mixes in the reactive C−H stretch and promotes cleavage of the C−H bond to produce CH_2D, in agreement with the simple spectator model.

Acknowledgment. We thank Professor Chan-Ho Kwon for his work on the redesign of the apparatus and Dr. Robert J. Holiday for advice about beginning this study. We gratefully acknowledge the support of this work by the National Science Foundation.

References and Notes

(1) Yoon, S.; Henton, S.; Zivkovic, A. N.; Crim, F. F. *J. Chem. Phys.* **2002**, *116*, 10744.
(2) Yoon, S.; Holiday, R. J.; Crim, F. F. *J. Chem. Phys.* **2003**, *119*, 4755.
(3) Yoon, S.; Holiday, R. J.; Sibert, E. L.; Crim, F. F. *J. Chem. Phys.* **2003**, *119*, 9568.
(4) Yoon, S.; Holiday, R. J.; Crim, F. F. *J. Phys. Chem. B* **2005**, *109*, 8388.
(5) Holiday, R. J.; Kwon, C. H.; Annesley, C. J.; Crim, F. F. *J. Chem. Phys.* **2006**, *125*, 133101.
(6) Simpson, W. R.; Rakitzis, T. P.; Kandel, S. A.; LevOn, T.; Zare, R. N. *J. Phys. Chem.* **1996**, *100*, 7938.
(7) Kandel, S. A.; Zare, R. N. *J. Chem. Phys.* **1998**, *109*, 9719.
(8) Kim, Z. H.; Bechtel, H. A.; Zare, R. N. *J. Am. Chem. Soc.* **2001**, *123*, 12714.
(9) Bechtel, H. A.; Kim, Z. H.; Camden, J. P.; Zare, R. N. *J. Chem. Phys.* **2004**, *120*, 791.
(10) Bechtel, H. A.; Camden, J. P.; Brown, D. J. A.; Zare, R. N. *J. Chem. Phys.* **2004**, *120*, 5096.
(11) Bechtel, H. A.; Camden, J. P.; Brown, D. J. A.; Martin, M. R.; Zare, R. N.; Vodopyanov, K. *Angew. Chem., Int. Ed.* **2005**, *44*, 2382.
(12) Kim, Z. H.; Bechtel, H. A.; Camden, J. P.; Zare, R. N. *J. Chem. Phys.* **2005**, *122*, 084303.
(13) Martin, M. R.; Brown, D. J. A.; Chiou, A. S.; Zare, R. N. *J. Chem. Phys.* **2007**, *126*, 044315.
(14) Zhou, J. G.; Lin, J. J.; Zhang, B. L.; Liu, K. P. *J. Phys. Chem. A* **2004**, *108*, 7832.
(15) Yan, S.; Wu, Y. T.; Liu, K. P. *Phys. Chem. Chem. Phys.* **2007**, *9*, 250.
(16) Yan, S.; Wu, Y. T.; Zhang, B. L.; Yue, X. F.; Liu, K. P. *Science* **2007**, *316*, 1723.
(17) Crim, F. F. *Proc. Nat. Acad. Sci. U.S.A.*, in press.
(18) Wiley, W. C.; McLaren, I. H. *Rev. Sci. Instrum.* **1955**, *26*, 1150.
(19) Brum, J. L.; Johnson III, R. D.; Hudgens, J. W. *J. Chem. Phys.* **1993**, *98*, 3732.
(20) Hudgens, J. W.; DiGiuseppe, T. G.; Lin, M. C. *J. Chem. Phys.* **1983**, *79*, 571.
(21) Andersen, F. A. *Mat.-Fys. Medd.* **1963**, *33*, 35.
(22) Blunt, V. M.; Brock, A.; Manzanares, C. *J. Phys. Chem.* **1996**, *100*, 4413.
(23) Lin, Z.; Boraas, K.; Reilly, J. P. *J. Mol. Spectrosc.* **1995**, *170*, 266.
(24) Lutz, B. L.; De Bergh, C.; Maillard, J. P. *Astrophys. J.* **1983**, *273*, 397.
(25) Tarrago, G.; Delaveau, M.; Fusina, L.; Guelachvili, G. *J. Mol. Spectrosc.* **1987**, *126*, 149.
(26) Herzberg, G. *Molecular Spectra and Molecular Structure: II. Infrared and Raman Spectra of Polyatomic Molecules*; Van Nostran Reinhold Co.: New York, 1945.
(27) Stakhursky, V. L.; Miller, T. A. SpecView: Simulation and Fitting Of Rotational Structure Of Electronic And Vibronic Bands. 56th Molecular Spectroscopy Symposium. (http://www.chemistry.ohio-state.edu/~vstakhur).
(28) Nikitin, A.; Brown, L. R.; Fejard, L.; Charnpion, J. P.; Tyuterev, V. G. *J. Mol. Spectrosc.* **2002**, *216*, 225.
(29) Holiday, R. J. Mode- and Bond-Selective Reaction of C-H Stretch Excited Monodeuterated Methane with Chlorine Atoms. Ph.D. Thesis, University of Wisconsin, Madison, 2006.

JP803901P